A Revised Model for Radial Profiles of Hurricane Winds

GREG J. HOLLAND

National Center for Atmospheric Research,* Boulder, Colorado

JAMES I. BELANGER AND ANGELA FRITZ

School of Earth and Atmospheric Sciences, Georgia Institute of Technology, Atlanta, Georgia

ABSTRACT

A revision to the Holland parametric approach to modeling the radial profile of winds in hurricanes is presented. The approach adopted uses information readily available from hurricane archives or in hurricane warning information and the profile can be readily incorporated into existing parametric models of the hurricane surface wind field. The original model utilized central and environmental surface pressures, maximum winds, and radius of maximum winds. In the revision a capacity to incorporate additional wind observations at some radius within the hurricane circulation was included. If surface observations are used, then a surface wind profile will result, obviating the need for deriving a boundary layer reduction from the gradient wind level. The model has considerably less sensitivity to data errors compared to the original and is shown to reproduce hurricane reconnaissance and surface wind profiles with high accuracy.

1. Introduction

Parametric radial profiles of hurricane winds form the basis of current approaches to assessing wind return periods and the development of engineering standards in hurricane-prone regions. In particular, the profile developed by Holland (1980, hereafter H80) has been used extensively for reconstructing hurricane wind fields, with various modifications, in a wide range of applications. Examples of this use include the following: engineering applications (Georgiou 1985; Vickery and Twisdale 1995; Vickery and Skerlj 2000; Powell et al. 2005); to drive a slab boundary layer model (Thompson and Cardone 1996; Vickery et al. 2009); to aid reconstruction of historical cyclones (Boose 2004); as a real-time analysis tool for surface winds (Xie et al. 2006); and for simulating ocean waves (Peng et al. 2006).

The use of such a simple approach is made possible by the remarkable consistency and relative uniformity of hurricane circulations, and indeed those of all intense vortices. As first noted by Leonardo da Vinci, all intense vortices are characterized by inward exponentially increasing winds to a maximum, then a rapid drop to a calm center. When normalized by the maximum wind and its radius, it is difficult to differentiate a radial profile of hurricane winds from an oceanic eddy, a tornado, or a wing-tip vortex. Uniformity is maintained by the manner in which perturbations that develop in the swirling flow are rapidly stretched by the strong shearing deformation, allowing the vortex swirl to retain its exponential shape (McWilliams 1984; Melander et al. 1988; Shapiro 2000).

Historical studies exploited this feature to construct an approximation of the full vortex circulation given only a small number of observed or estimated parameters. Our purpose here is to present an updated version of the H80 radial wind model that removes some difficulties with the original, including the dependence on an accurate knowledge of the maximum winds and their radius and the lack of a straightforward way of fitting the outer and inner winds' version, and that can more readily accommodate modern observing system data. In doing this, we follow the principles adopted in the revised pressure wind relationship developed in Holland (2008, hereafter H08).

H08 specifically addresses determination of the b parameter. Further improvements to the radial wind model that are made here include

- Improved ability to accommodate both external and core wind observations;
- Reduced dependence on an accurate knowledge of the radius of maximum winds;
- Capacity to handle bimodal wind profiles associated with secondary eyewall generation; and
- Reduced issues with lack of resolution in some cyclones in the vicinity of the maximum winds, which can lead to an underestimate of the true maximum winds, or an overestimate of external winds if the core is artificially enhanced (H80).

We are only interested in upgrading the analytic representation of the radial profile of hurricane winds in a manner that can be readily applied to a wide variety of hurricane profile shapes and in ensuring that this method has low sensitivity to observing system errors in the underlying parameters; the choice of approach to development of the full 2D wind field is left to the user of the profile. The revised wind model can be easily substituted for H80 in existing hurricane wind field models.

A brief background to radial wind profiles is presented in section 2, together with the two profiles that we will use for comparison with the new profile. Section 3 describes the new radial profile, together with an analysis of sensitivity to errors and application to real data. Section 4 presents a comparison of the model to real data and our conclusions are presented in section 5.

2. Previous approaches

Historical examples of parametric radial profiles that have been used in hurricane applications include the Rankine combined vortex approximation (named after the Scottish engineer, William Rankine) and the rectangular hyperbola approximation to the associated surface pressure field first proposed by Schloemer (1954) and extended by H80.

A Rankine combined vortex consists of a region of solid-body rotation, or constant vorticity, at the center surrounded by a circulation with zero vorticity:

$$v = v_m\left(\frac{r}{r_{v_m}}\right) \quad r < r_{v_m},$$
$$= v_m\left(\frac{r_{v_m}}{r}\right)^x \quad r \geq r_{v_m}, \qquad (1)$$

where v_m are the maximum winds, r_{v_m} is the radius of maximum winds, and x is a scaling parameter that

adjusts the profile shape (Depperman 1947). Although a pure Rankine vortex set is $x = 1$, smaller values are normally used to accommodate the angular momentum loss by surface friction in a typical hurricane. Following Riehl (1954), we use $x = 0.5$.

Schloemer (1954) suggested that the radial surface pressure profile can be approximated by a rectangular hyperbola, which then can be differentiated to find the wind speed. H80 showed that an improved relationship could be obtained by use of a modified rectangular hyperbola of the following form:

$$p_s = p_{cs} + \Delta p_s e^{-\left(\frac{r_{v_m}}{r}\right)^b}, \qquad (2)$$

where p_s is the surface pressure at radius r; p_{cs} is the central pressure; $\Delta p_s = p_{ns} - p_{cs}$ is the pressure drop from a defined external pressure p_{ns} to the cyclone center; and e is the base of natural logarithms. The exponent b is a scaling parameter that defines the proportion of pressure gradient near the maximum wind radius, or alternatively the maximum wind speed for a given pressure drop. Using (2) in the cyclostrophic wind equation leads to

$$v_c = \left[\frac{100b\Delta p_s\left(\frac{r_{v_m}}{r}\right)^b}{\rho e^{\left[\frac{r_{v_m}}{r}\right]^b}}\right]^{0.5} \quad \text{or}$$
$$v_c = v_m\left\{\left(\frac{r_{v_m}}{r}\right)^b e^{\left[1-\left(\frac{r_{v_m}}{r}\right)^b\right]}\right\}^{0.5}, \qquad (3)$$

where v_c is the cyclostrophic wind, v_m is the maximum wind at the gradient level (in m s^{-1}), Δp_s (in hPa), and the air density ρ (in kg m^{-3}) at the gradient level.

Several other wind profile relationships have been developed for specific purposes, two of which we shall make use of for comparative purposes. The first profile follows Emanuel (2004):

$$v^2 = v_m^2\left(\frac{r_0 - r}{r_0 - r_{v_m}}\right)^2\left(\frac{r}{r_{v_m}}\right)^{2m}$$
$$\times\left\{\frac{(1-a)(n+m)}{n+m\left(\frac{r}{r_{v_m}}\right)^{2(n+m)}} + \left[\frac{a(1+2m)}{1+2m\left(\frac{r}{r_{v_m}}\right)^{2m+1}}\right]\right\}, \qquad (4)$$

where r_0 is a large radius where the vortex perturbation drops to zero; and a, n, m are scaling parameters. Following Emanuel et al. (2006) we set $r_0 = 1200$ km, $a = 0.25$, $m = 1.6$, and $n = 0.9$ for this study. The second radial wind profile is from DeMaria (1987):

$$v = \frac{rv_m}{r_{v_m}} e^{\left[1-\left(\frac{r}{r_{v_m}}\right)^c\right]/d}, \quad (5)$$

where c is a scaling parameter similar to b in (3), and d is another empirical parameter, which we set to 1 following Leslie and Holland (1995).

A number of other radial wind profiles exist (e.g., Willoughby et al. 2006; Fujita 1952) but are not considered further here. The Willoughby et al. profile has been shown to be able to accurately fit known profiles.

3. The revised radial wind profile

a. Derivation

We retain the rectangular hyperbolic form of the radial pressure variation in (2), although the explicitly derived form of the radial variation of winds is empirically adjusted from the previous version in (3). First, we follow the principle used in H08 and eliminate the intermediate step of first calculating the gradient level flow and then reducing this field to the surface. Rather we generalize the formulation to incorporate observations of winds at any level (e.g., surface or flight level). Second, we allow a variable exponent in (3) to accommodate both the maximum wind assessments and data in the outer circulation. Thus, (3) becomes

$$v_s = \left[\frac{100b_s \Delta p_s \left(\frac{r_{v_{ms}}}{r}\right)^{b_s}}{\rho_s e^{\left(\frac{r_{v_m}}{r}\right)^{b_s}}}\right]^x \quad \text{or}$$

$$v_s = v_{ms} \left\{\left(\frac{r_{v_{ms}}}{r}\right)^{b_s} e^{\left[1-\left(\frac{r_{v_{ms}}}{r}\right)^{b_s}\right]}\right\}^x, \quad (6)$$

where the subscript s refers to surface values (at a nominal height of 10 m). Parameter b_s is related to the original b by $b_s = bg_s^x$, where g_s is the reduction factor for gradient-to-surface winds. If we set $x = 0.5$ and keep b_s constant following H80, then it is often impossible to accurately reproduce both the core and external wind structure in hurricanes (e.g., Willoughby and Rahn 2004). Allowing x and/or b_s to vary with radius substantially improves this reproduction. We experimented with various combinations of varying x and b_s and settled on keeping b_s constant and allowing x to vary linearly. Hence, application of (6) requires the following data: the central pressure (with or without maximum winds), radius of maximum winds, an external pressure and collocated surface wind speed, and surface air density.

If the maximum surface winds and central pressure have been directly or reliably independently observed, then we can estimate the b_s parameter (following H80) by

$$b_s = \frac{v_{ms}^2 \rho_{ms} e}{100(p_{ns} - p_{cs})}. \quad (7)$$

However, if the analysis uses Dvorak or other remote assessment, we recommend the approach adopted by H08 of estimating the central pressure first and then deriving the b_s parameter and v_{ms}:

$$b_s = -4.4 \times 10^{-5} \Delta p_s^2 + 0.01 \Delta p_s + 0.03 \frac{\partial p_{cs}}{\partial t}$$
$$-0.014\varphi + 0.15v_t^x + 1.0,$$
$$x = 0.6\left(1 - \frac{\Delta p_s}{215}\right), \quad \text{and}$$
$$v_{ms} = \left(\frac{100b_s}{\rho_{ms} e} \Delta p_s\right)^{0.5}, \quad (8)$$

where Δp_s in hPa, $\partial p_{cs}/\partial t$ the intensity change in hPa h^{-1}; φ is the absolute value of latitude in degrees; and v_t the cyclone translation speed in m s^{-1}.

The surface air density can be derived to good approximation by (H08)

$$\rho_s = \frac{100p_s}{RT_{vs}},$$
$$T_{vs} = (T_s + 273.15)(1 + 0.61q_s),$$
$$q_s = \text{RH}_s\left(\frac{3.802}{100p_s}\right)e^{\frac{17.67T_s}{243.5+T_s}}, \quad \text{and} \quad (9)$$
$$T_s = \text{SST} - 1,$$

where $R = 286.9$ J kg^{-1} K^{-1} is the gas constant for dry air, T_{vs} is the virtual surface temperature (in K), q_s is the surface moisture (in g kg^{-1}), T_s is the surface temperature and SST is the sea surface temperature (both in °C), and RH$_s$ is the surface relative humidity (assumed at 0.9 in the absence of direct observations). Thus, the only external input required in (9) is an estimate of the SST and the surface pressure from (2). This enables an improved fit with error reduction of several percent for intense cyclones. However, it is not critical and a constant value of density can be used if preferred. Alternatively if there is a good estimate of the maximum winds, then the alternate method in (6) can be used as it does not require an explicit estimate of the density.

Next we need to determine the variation in the exponent of (3). First we keep $x = 0.5$ for $r \le r_{v_m}$ for consistency with H08, and this will be shown a posteriori to be unimportant. We could adjust the profile using least squares to observed winds at various radii by an iterative solution of (3) to provide a functional form of x. For general purposes, however, such information is not readily available so we assume a linear variation of x with radius:
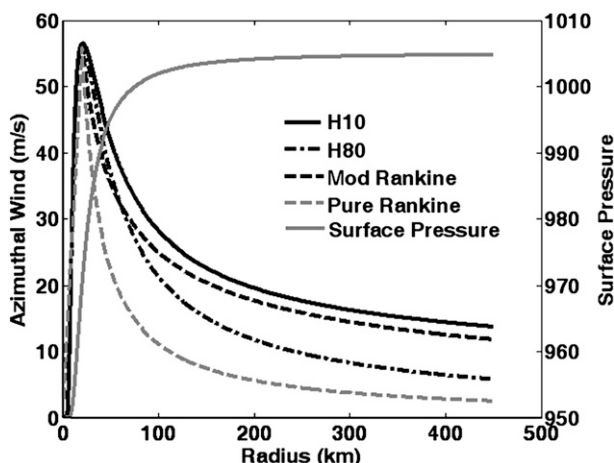
FIG. 1. Profiles for the standard hurricane defined in the text: the revised wind profile (H10), the original profile of H80, and (left axis) both the modified and original Rankine vortex profiles, and (right axis) the surface pressure profile.

$$x = 0.5 \qquad\qquad r \le r_{v_m},$$
$$x = 0.5 + (r - r_{v_m})\frac{x_n - 0.5}{r_n - r_{v_m}} \quad r > r_{v_m}, \tag{10}$$

with x_n being the adjusted exponent to fit the peripheral observations at radius r_n.

Equations (2) and (6)–(10) define the revised wind profile model. Two points are noted:

- The wind field thus derived is both at the surface and empirically adjusted; therefore, it will not be in gradient balance with the surface pressure profile. Should there be a need for a pressure profile, then this can still be derived from the original pressure formulation in (2). It will provide the same good pressure fit but will not be in exact balance with the winds. If a gradient-level wind is required (e.g., to enable application of a boundary layer model to estimate the surface winds), this can be achieved by applying the wind model directly to gradient-level observations.
- The wind profile is not necessarily just the azimuthal flow; if observations of the total flow are used, the profile will represent total winds (including the radial component).

b. Structure and sensitivity analysis

As a basis for an overall discussion on structure and sensitivity to basic parameters, we adopt a baseline hurricane composed of the following: $p_{ns} = 1005$ hPa, $v_{ns} = 17$ m s^{-1} (the peripheral wind observation used in fitting the profile), $r_n = 300$ km, $p_{cs} = 950$ hPa, $r_{v_{ms}} = 20$ km, SST = 28°C, $\partial p_{cs}/\partial t = 3$ hPa s^{-1}, $\varphi = 20°$, and $v_t = 5$ m s^{-1}. From (8) these parameters result in values of $b_s = 1.8$ and $v_{ms} = 56$ m s^{-1}. The resulting wind profile (H10 in Fig. 1) is a marked improvement on the older
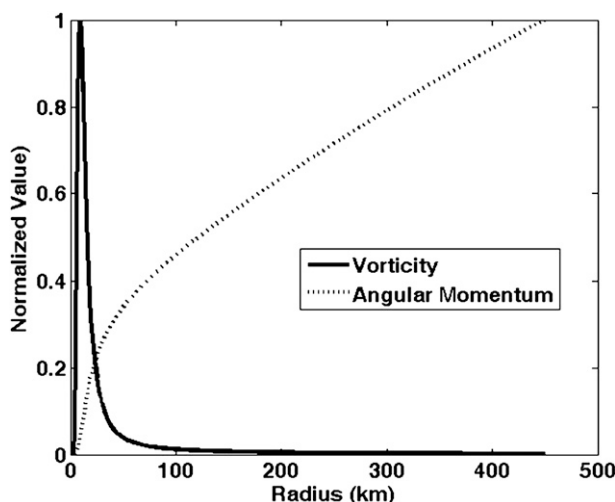

FIG. 2. Relative vorticity and angular momentum profiles, normalized by their maxima.

(H80) version, in that the profile now passes through both the defined maximum and peripheral winds. For the H80 model, a close fit to the maximum wind would have led to a marked underestimate of the outer circulation. On this occasion the modified Rankine vortex also would have been a good fit, but that is by chance. Derived parameters shown in Fig. 2 indicate that the model has standard physical characteristics of a stable profile of angular momentum increasing with radius and a vortex ring in the maximum wind zone.

The overall sensitivity to errors in the specified input parameters is investigated in Fig. 3. The sensitivity analysis was conducted by randomly applying 50 changes drawn from within one standard deviation of a normal distribution, as indicated by the error range in each panel.

Errors in specifying the maximum winds (Fig. 3a) are largely confined to the vicinity of the maximum winds and have a minor impact on the outer circulation. This is a result of the constraint on the profile passing through the outer wind observations and is a substantial improvement on H80. A similar effect is seen for errors in the radius of maximum winds (Fig. 3b), and even errors of up to 50% in this radius result in relatively small errors in the overall wind profile. Both of these changes do produce an amplified response inside the eye as a result of the locally strong gradients.

By comparison, errors in specifying the outer wind parameters tend to extend through much of the profile (Figs. 3c,d), although large errors in these parameters are required to have a marked impact on the total wind field. This means that archived values of the subjectively defined radius of the outer closed isobar, or gale-force winds, can likely be used to good effect, as can scatterometer data. Note in Fig. 3d that the profile errors resulting from
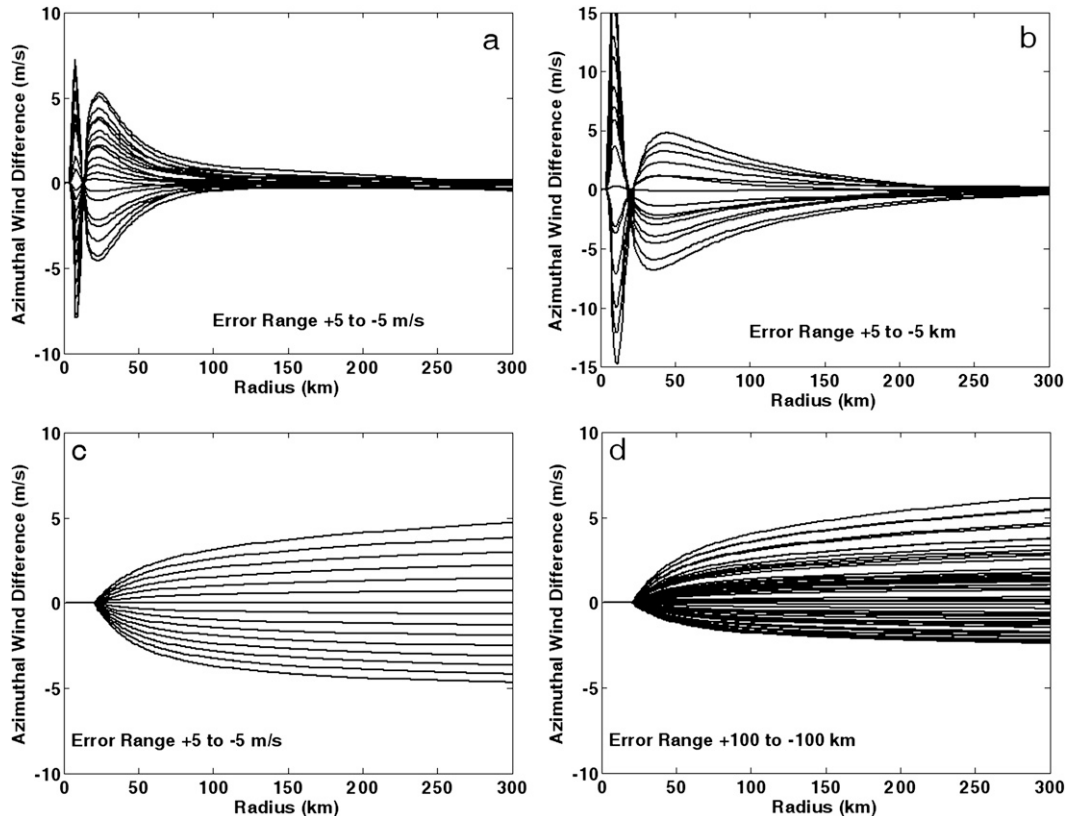
FIG. 3. Sensitivity to randomly applied pseudoerrors drawn from a normal distribution with the range of the errors indicated: (a) maximum winds, (b) radius of maximum winds, (c) outer wind, and (d) radius of outer wind. In (a)–(d), the ordinate is the change in azimuthal winds from the base profile, with positive indicating the perturbed profile is higher than the base and vice versa.

placing the outer observation at larger radii are greater than for an equivalent displacement inward.

The lack of sensitivity to maximum wind radius is of considerable benefit when applying profiles to archived storms, for which the maximum wind radius is often not known and is normally unobtainable before the satellite era. If some external wind observation is available, then Fig. 3b indicates that using a generic maximum wind radius at around the mean for the region will still enable a reasonable assessment of the overall wind profile to be made, especially if there is some independent estimate of the central pressure. Of course, Figs. 3c,d do show that this will only work reasonably if the outer wind observation is not substantially in error from incorrect location or speed.

c. Secondary wind maxima

A number of severe hurricanes develop secondary wind maxima that evolve in time, usually migrating inward to displace and finally replace the original maximum (e.g., Willoughby et al. 1982). There are several ways in which the standard profile can be modified to

accommodate these cases. We adopt the straightforward approach of adding a perturbation that has similar characteristics to the primary wind profile. This requires only an estimate of the secondary wind maximum, its radius, and the radial extent of the perturbation.

The maximum perturbation wind v_{msp} is obtained by taking the secondary wind maximum and subtracting the wind value from the standard profile at the same radius. Next we calculate a perturbation pressure change, Δp_{sp}, from the outer radius of the perturbation to the inner using a rearranged (3) with $x = 0.5$ and $r_m = r$ to obtain the following:

$$\Delta p_{sp} = \frac{v_{msp}^2 \rho_s e}{100 b_s}. \tag{11}$$

A wind perturbation is then developed using (6)–(10) but using the perturbation quantities. Finally, this perturbation is added back to the original wind profile, with some minor smoothing to ensure an even fit at the extremities. Figure 4 shows an example of applying a 40 m s^{-1} secondary wind maximum at 100-km radius with
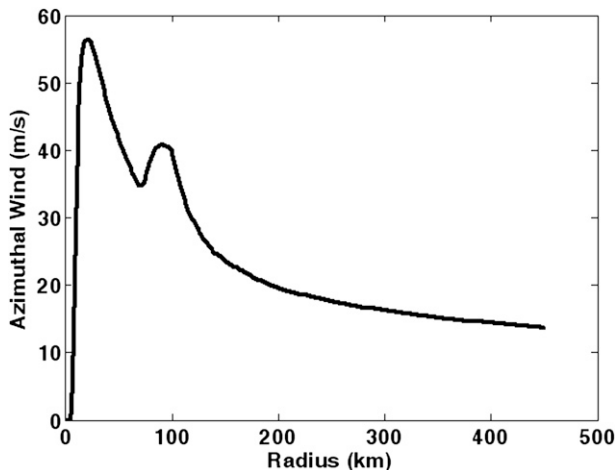
FIG. 4. Result of adding a secondary wind maximum of 40 m s^{-1} at a radius of 100 km to the wind profile in Fig. 1 with the total perturbation constrained between 60 and 150 km.

the perturbation constrained between 60 and 150 km to the standard hurricane profile. This approach can be applied to multiple secondary maxima if required.

Care should be taken in applying this approach if dynamical instabilities are an issue (e.g., for model bogus applications). Applying a large perturbation may result in a change of vorticity gradient and resulting barotropic instability.

4. Application to observations

a. Aircraft reconnaissance data

Figure 5 shows the degree to which the present model (hereafter referred to as H10), Emanuel's model in (4), and DeMaria's model in (5) can reproduce aircraft reconnaissance data. The observations are from 457 aircraft reconnaissance flight-level profiles for six North Atlantic

hurricanes representing a range of sizes and intensities: Iris (1995), Opal (1995), Georges (1998), Mitch (1998), Floyd (1999), and Michelle (2001). The data were obtained from a National Oceanic and Atmospheric Administration (NOAA) Hurricane Research Division project that processed the data in terms of distance from the storm center as well as the storm quadrant and are in storm-relative coordinates (Willoughby et al. 1982). For this exercise, we produce H10 profiles directly at flight level by fitting to the maximum and outer-flight-level wind observations. Both the wind profile and reconnaissance data are binned into 5-km intervals and then normalized by the r_{v_m}. Thus, the first bin includes wind data from r_{v_m} to r_{v_m} + 5 km, the second from r_{v_m} + 6 km to r_{v_m} + 10 km, and so on. There are 30 possible bins since the flight-level profiles extend out to a maximum radius of 150 km. Model performance is evaluated using linear correlation, bias, and root-mean-square error (RMSE) compared to the aircraft data for each RMW-relative "bin." Statistical significance is determined using a two-sided t test of the null hypothesis that the correlation is due to random chance alone.

Figure 5a shows the linear correlation between all of the flight and H10 profiles as the dark, solid line. The correlation is statistically significant at the 99% level for all bins and has a minimum at bin 8. The average correlation is 0.82, indicating that H10 explains 67% of the variance in the flight-level data across all 457 flight level profiles. This means that H10 is quite good at capturing variations between radial profiles, including the intensity, size and varying profile shapes. Bias in applying H10 (Fig. 5b) has a maximum of 4 m s^{-1} near bins 1–2. The average for the whole profile is just over 1 m s^{-1}, and the bias at any bin is typically less than 10% of the observed wind. The RMSE for each radial bin (Fig. 5c) is low at all locations beyond r_{v_m}, with a maximum RMSE of around 6 m s^{-1} at bin 2 and a minimum of 2.6 m s^{-1} at bins 10–11.
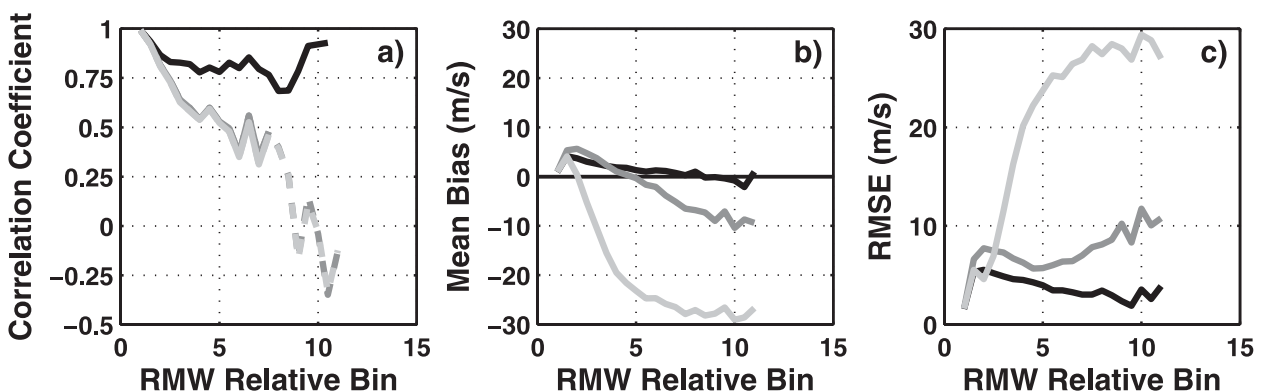

FIG. 5. Results of application of H10 (black), Emanuel in (4) (dark gray), and DeMaria in (5) (light gray) to 457 Atlantic reconnaissance profiles for (a) linear correlation, (b) bias (m s^{-1}), and (c) rmse (m s^{-1}). Significance at the 99% level is denoted by the solid part of the line in (a).
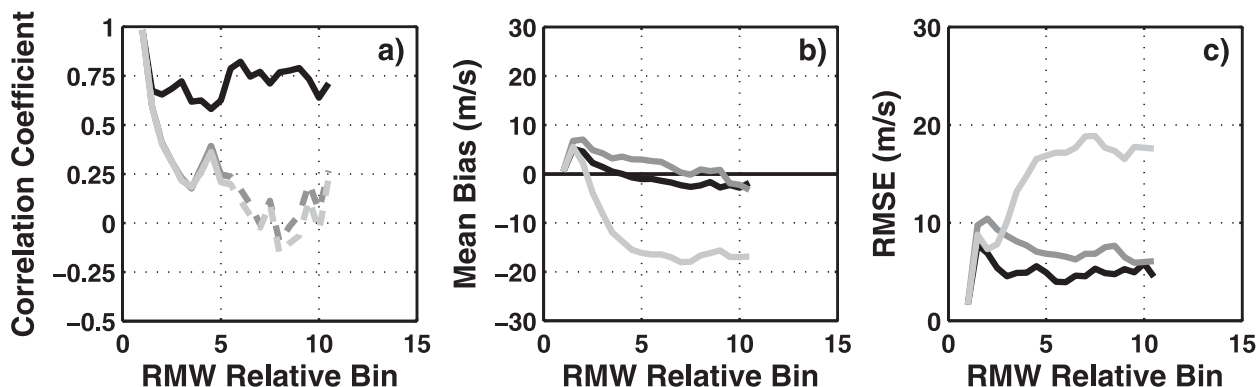
FIG. 6. Results of application of H10 (black), Emanuel in (4) (dark gray), and DeMaria in (5) (light gray) to 121 Atlantic SFMR surface wind profiles for (a) linear correlation, (b) bias (m s^{-1}), and (c) rmse (m s^{-1}). Significance at the 99% level is denoted by the solid part of the line in (a).

The overall profile of the error statistics validates our choice of a linear variation of the exponent, x, in (6). There is little evidence of major variation in errors across the domain and across a wide range of profiles. We next compare H10 with Emanuel's model in (4) and DeMaria's model in (5). Out to bin 2, the correlations for (4) and (5) are comparable to H10 (Fig. 5a), an expected result since all profiles use maximum winds as an input parameter. At larger radii both (4) and (5) are unable to capture a majority of the observed variance in the flight-level data, and the fit becomes statistically insignificant at outer radii. The average variance explained across all radial bins is 19% for (5) and 20% for (4), compared to 67% for H10. Model bias (Fig. 5b) is slightly positive for (4) over most of the domain and is similar to H10, except in the outer region, where it becomes negative and >5 m s^{-1}. Equation (5) has a large negative bias across most of the domain and exceeds 25 m s^{-1} at the outer radii. Both H10 and (4) outperform (5) in terms of model bias. RMSE (Fig. 5c) is comparable for all models out to bins 2–3. At larger radii, the RMSE decreases steadily for H10 to 2 m s^{-1}, whereas (4) remains steady and then increases sharply, and (5) increases linearly to >25 m s^{-1}. These results demonstrate the usefulness of anchoring the wind profile at some outer observation as well as at the radius of maximum winds.

b. Stepped frequency microwave radiometer surface data

Data from the stepped frequency microwave radiometer (SFMR; Uhlhorn et al. 2007) on hurricane reconnaissance aircraft in the North Atlantic provide a method of comparing the surface wind version of H10 directly with observations. The SFMR data in this analysis were provided courtesy of the NOAA/Hurricane Research Division's archive of Air Force reconnaissance flights during the 2008 hurricane season. A total of 11 tropical cyclones were processed for wind

profiles including: Bertha, Cristobal, Dolly, Edouard, Fay, Gustav, Hanna, Ike, Kyle, Omar, and Paloma.

The analysis was restricted to SFMR data from within 300 km of the cyclone center and the center fix was determined using the Hurricane Database (HURDAT) 6-h location coordinates linearly interpolated to nearest 1 min. Unique wind profiles were determined by identifying inflection points in the SFMR distance from the tropical cyclone (TC) center data with a requirement that each profile had at least 5 min of time separation. Since the SFMR data has a high temporal and spatial resolution, a 35-point running mean was applied to each profile, which is roughly equivalent to smoothing to the 5-km bins used for the aircraft flight data. The following postprocessing steps were then taken before the profiles were used in the final analysis:

- The profile data must have a maximum wind of at least 33 m s^{-1} (hurricane strength or greater);
- The radial wind profile must extend at least 150 km; and
- To account for questionable SFMR wind profiles, we required that $10 < r_{v_{ms}} < 70$ km.

Some assumptions were required in applying H10, since the SFMR data alone do not contain temperature, moisture, or pressure information. First, we assumed the mean temperature of the environment was 28°C, the relative humidity was fixed at 90%, the central pressure was the nearest 6-h minimum pressure assigned in HURDAT, and a standard environmental pressure of 1020 hPa was used.

In total, 121 wind profiles from the 2008 hurricane season were thus included in the SFMR verification analysis. The results in Fig. 6 are consistent with the verification analysis using flight-level wind data. We find that H10 is superior especially in reproducing the outer surface-wind profile of the tropical cyclone in comparison to the Emanuel and DeMaria models. H10 provided moderate to high correlation coefficients at all bins and

low mean bias and root-mean-square error, especially from bins 5–10. In comparison to the flight-level verification, H10 does not perform as well in reproducing the SFMR profile data, but this difference is likely due to the key assumptions that were made in constructing the profiles (i.e., assuming mean temperature, relative humidity, and a standard environmental pressure).

In summary, the verification analysis using both aircraft flight-level wind data and SFMR data provides robust evidence that H10 can be used to confidently reconstruct wind profiles in hurricanes.

5. Conclusions

We have developed a revised version of the H80 parametric radial profile of hurricane winds by allowing a variation in the wind equation exponent to fit to inner and outer wind observations. Input data consist of an outer wind and surface pressure, sea surface temperature, radius of maximum winds, and central pressure. All of these parameters are readily available from most hurricane archives or warnings. If both maximum winds and central pressure are independently measured, then either or both may be used. Furthermore, the profile can be applied directly at the surface, or at any level for which observations are available, obviating the need in H80 for using some form of boundary layer reduction to derive a surface wind from a gradient level profile. Secondary wind maxima can be included by adding a perturbation with specified amplitude and radial range to the standard profile.

The revised model is dynamically stable and has a damped response to errors in the input data. It provides an accurate fit to observed hurricane reconnaissance observations for a range of North Atlantic hurricanes. For the 457 reconnaissance legs used, the model explained 67% of the variance, produced a bias of <10% at all radii, and was demonstrated to be an improvement on two other wind profile models. A similar result was obtained for application to surface SFMR data.

By retaining much of the original model, changes to existing techniques based on this model can be accommodated with minimal effort. The revised model also can be applied with similar numerical efficiency, enabling massive numbers of simulations for catastrophe modeling statistics. If there are several observations around the periphery of a hurricane [e.g., from the Quick Scatterometer (QuikSCAT)], then a series of profiles can be produced and then analyzed to produce a full surface wind field. Alternatively a symmetric, gradient-level vortex can be produced for use in driving a slab boundary layer model to arrive at a surface wind field.

We suggest that existing systems, models, and procedures using the H80 model adopt this revised parametric approach. We have retained the basic characteristics of the original model, so required changes to code and approach will be minimal. The end result should be more accurate, robust, and less prone to errors in any of the input parameters. If no direct external wind observations are available, then an estimate of the radius of gale-force winds will suffice. As shown in Fig. 3d, errors in this radius will not have a marked effect on the accuracy of the wind field, whereas the anchoring of the profile in the outer domain will produce a marked improvement.

REFERENCES

Boose, E. R., 2004: A Method for reconstructing historical hurricanes. *Hurricanes and Typhoons: Past, Present, and Future,* R. Murnane and K. Liu, Eds., Columbia University Press, 99–120.

DeMaria, M., 1987: Tropical cyclone track prediction with a barotropic spectral model. *Mon. Wea. Rev.,* **115,** 2346–2357.

Depperman, R. C. E., 1947: Notes on the origin and structures of Philippine typhoons. *Bull. Amer. Meteor. Soc.,* **28,** 399–404.

Emanuel, K. A., 2004: Tropical cyclone energetics and structure. *Atmospheric Turbulence and Mesoscale Meteorology,* E. Federovich, R. Rotunno, and B. Stevens, Eds., Cambridge University Press, 165–192.

——, S. Ravela, E. Vivant, and C. Risi, 2006: A statistical-deterministic approach to hurricane risk assessment. *Bull. Amer. Meteor. Soc.,* **87,** 299–314.

Fujita, T., 1952: Pressure distribution within a typhoon. *Geophys. Mag.,* **23,** 437–451.

Georgiou, P., 1985: Design wind speeds in tropical cyclone prone regions. Ph.D. thesis, University of Western Ontario, 295 pp.

Holland, G., 1980: An analytic model of the wind and pressure profiles in hurricanes. *Mon. Wea. Rev.,* **108,** 1212–1218.

——, 2008: A revised hurricane pressure–wind model. *Mon. Wea. Rev.,* **136,** 3432–3445.

Leslie, L. M., and G. J. Holland, 1995: On the bogussing of tropical cyclones in numerical models: A comparison of vortex profiles. *Meteor. Atmos. Phys.,* **56,** 101–110.

McWilliams, J. C., 1984: The emergence of isolated coherent vortices in turbulent flow. *J. Fluid Mech.,* **146,** 21–43.

Melander, M. V., N. J. Zabusky, and J. C. McWilliams, 1988: Symmetric vortex merger in two dimensions: Causes and conditions. *J. Fluid Mech.,* **195,** 303–340.

Neumann, C. J., B. R. Jarvinen, C. J. McAdie, and G. R. Hammer, 1999: Tropical cyclones of the North Atlantic Ocean, 1871–1998. NOAA, 206 pp.

Peng, M., L. Xie, and L. J. Pietrafesa, 2006: Tropical cyclone induced asymmetry of sea level surge and fall and its presentation in a storm surge model with parametric wind fields. *Ocean Modell.,* **14,** 81–101.

Powell, M. D., G. Soukup, S. Cocke, S. Gulati, N. Morisseau-Leroy, S. Hamid, N. Dorst, and L. Axe, 2005: State of Florida hurricane

loss prediction model: Atmospheric science component. *J. Wind Eng. Ind. Aerodyn.,* **93,** 651–674.

Riehl, H., 1954: *Tropical Meteorology*. McGraw-Hill, 392 pp.

Schloemer, R. W., 1954: Analysis and synthesis of hurricane wind patterns over Lake Okeechobee, Florida. Hydrometeorological Rep. 31, Department of Commerce and U.S. Army Corps of Engineers, U.S. Weather Bureau, Washington, DC, 49 pp.

Shapiro, L. J., 2000: Potential vorticity asymmetries and tropical cyclone evolution in a moist three-layer model. *J. Atmos. Sci.,* **57,** 3645–3662.

Thompson, E. F., and V. J. Cardone, 1996: Practical modeling of hurricane surface wind fields. *J. Waterway Port Coastal Ocean Eng.,* **122,** 195–205.

Uhlhorn, E. W., P. G. Black, J. L. Franklin, M. Goodberlet, J. Carswell, and A. S. Goldstein, 2007: Hurricane surface wind measurements from an operational stepped frequency microwave radiometer. *Mon. Wea. Rev.,* **135,** 3070–3085.

Vickery, P. J., and L. A. Twisdale, 1995: Wind-field and filling models for hurricane wind-speed predictions. *J. Struct. Eng.,* **121,** 1700–1709.

——, and P. F. Skerlj, 2000: On the elimination of exposure D along the hurricane coastline in ASCE-7. *J. Struct. Eng.,* **126,** 545–549.

——, D. Wadhera, M. D. Powell, and Y. Chen, 2009: A hurricane boundary layer and wind field model for use in engineering applications. *J. Appl. Meteor. Climatol.,* **48,** 381–405.

Willoughby, H. E., and M. E. Rahn, 2004: Parametric representation of the primary hurricane vortex. Part I: Observations and evaluation of the Holland (1980) model. *Mon. Wea. Rev.,* **132,** 3033–3048.

——, J. A. Clos, and M. G. Shoreibah, 1982: Concentric eye walls, secondary wind maxima, and the evolution of the hurricane vortex. *J. Atmos. Sci.,* **39,** 395–411.

——, R. W. R. Darling, and M. E. Rahn, 2006: Parametric representation of the primary hurricane vortex. Part II: A new family of sectionally continuous profiles. *Mon. Wea. Rev.,* **134,** 1102–1120.

Xie, L., S. Bao, L. J. Pietrafesa, K. Foley, and M. Fuentes, 2006: A real-time hurricane surface wind forecasting model: Formulation and verification. *Mon. Wea. Rev.,* **134,** 1355–1370.